

1
2
3
4
5
6
7
8
9
10
11
12
13
14
15
16
17
18
19
20
21

Supplemental information

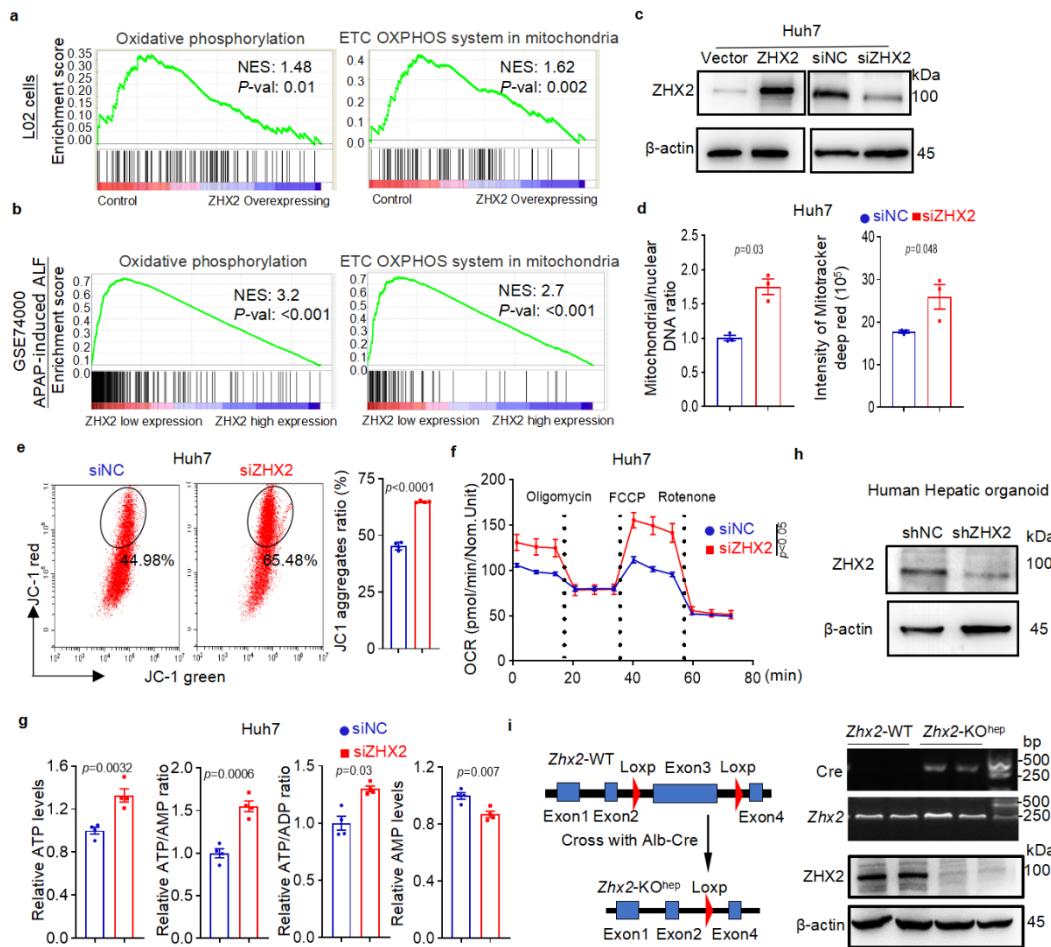
ZHX2 emerges as a negative regulator of mitochondrial oxidative phosphorylation during acute liver injury

This file includes:

Supplementary Figures 1 to 7

Supplementary Tables 1 to 2

22 **Supplementary Figures and Figure legends**



23

24 **Supplementary Figure 1. ZHX2 inhibits mitochondrial OXPHOS *in vitro* and *in vivo*.**

25 **a-b** GSEA analysis were performed with publicly available data, including ZHX2-

26 overexpressed LO2 cells, APAP-induced acute liver failure (ALF) (GSE74000), respectively.

27 NES, normalized enrichment score, $P < 0.05$ was considered statistically significant. Data

28 were analyzed using Kolmogorov-Smirnov test. **c** Western blot analysis for ZHX2 in Huh7

29 cells with ZHX2 ectopic expression or knockdown. These experiments have been

30 repeated for three times with similar results. **d** Detection of copy number of mtDNA (left)

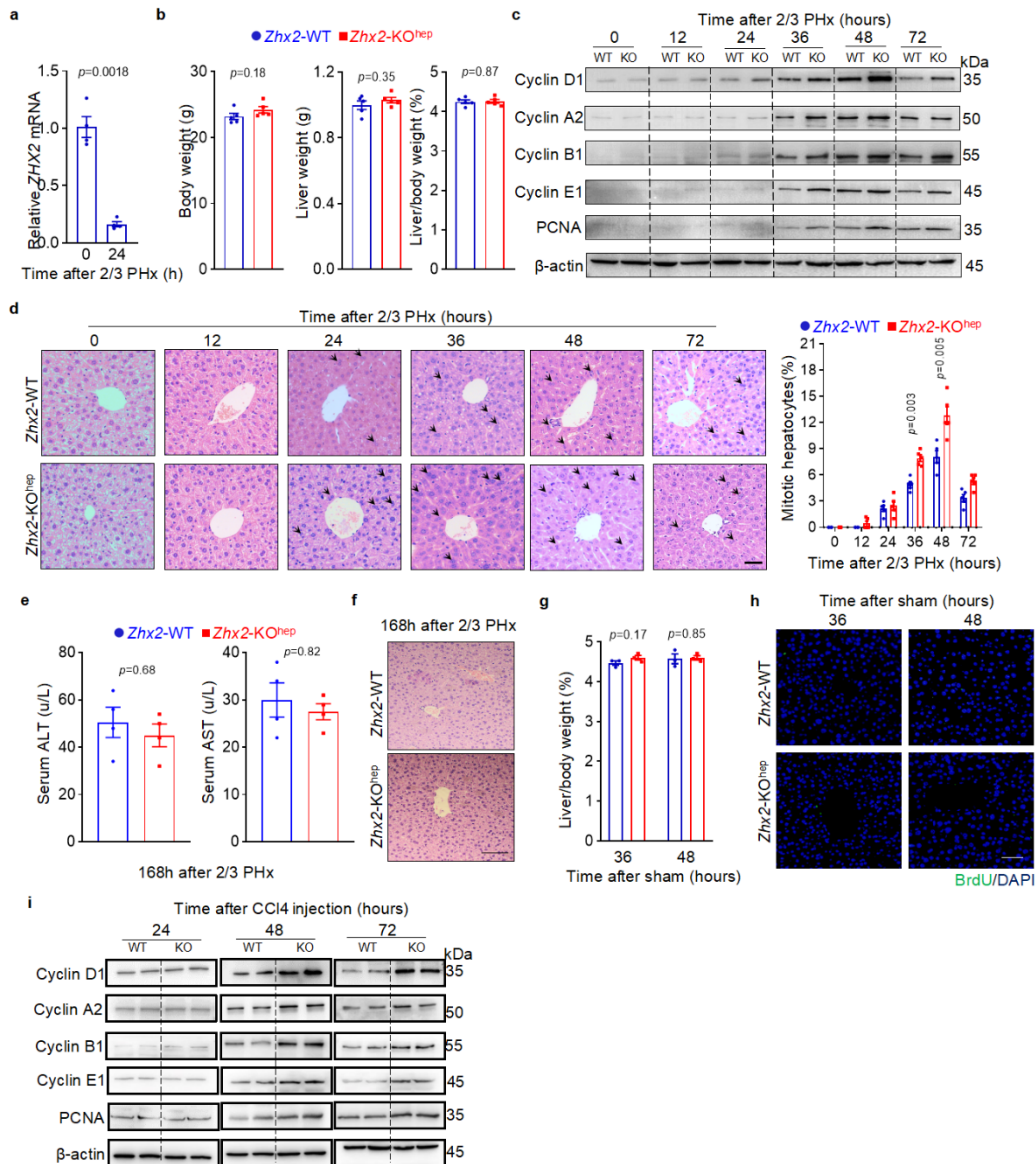
31 and intensity of Mito tracker deep red (right) in Huh7 cells with or without ZHX2 knockdown,

32 respectively. Representative data are presented as mean \pm sd. (Two-tailed Student's t test.

33 n=3 biologically independent samples). **e** Fluorescence intensity of JC-1 in Huh7 cells with
34 or without ZHX2 knockdown were analyzed by flow cytometry. Representative flow
35 cytometry plots are presented in the left panel. Histograms display the quantitative data in
36 the right panel. Representative data are presented as mean \pm sd. (Two-tailed Student' s t
37 test. n=4 biologically independent samples). **f** Relative oxygen consumption rate was
38 measured siNC and siZHX2 transfected Huh7 cells by seahorse analyzer. The data were
39 normalized to protein abundance. Representative data are presented as mean \pm sd. (Two-
40 tailed Student' s t test. n=3 biologically independent samples). **g** Levels of ATP and AMP,
41 and ratios of ATP/AMP and ATP/ADP were determined in Huh7 cells transfected with siNC
42 and siZHX2. Representative data are presented as mean \pm sd. (Two-tailed Student' s t test.
43 n=4 biologically independent samples). **h** Western blot analysis for knockdown efficiency
44 of ZHX2 in human hepatic organoid. These experiments have been repeated for three
45 times with similar results. **i** Establishment of liver-specific ZHX2 knockout mice were
46 confirmed. Schematic diagram of *Zhx2*-KO^{hep}(left) is presented (Left). Mouse tails were
47 collected to extract DNA for genotyping by PCR (Top right). ZHX2 protein levels were
48 detected in *Zhx2*-WT and *Zhx2*-KO^{hep} mice liver tissues by western blot (Bottom right).

49

50



51

52 **Supplementary Figure 2. Hepatic *Zhx2* deficiency enhances liver repair in 2/3 PHx**
 53 **and CCl4-induced liver injury.**

54 **a** ZHX2 expression was determined in wild type mouse liver at 0 and 24 h after 2/3 PHx

55 and by RT-qPCR. Data are presented as mean \pm s.e.m. (Two-tailed Student' s t test. n=4

56 mice per group). **b** Liver weight, body weight, and the liver/body weight ratios of 8-10-week-

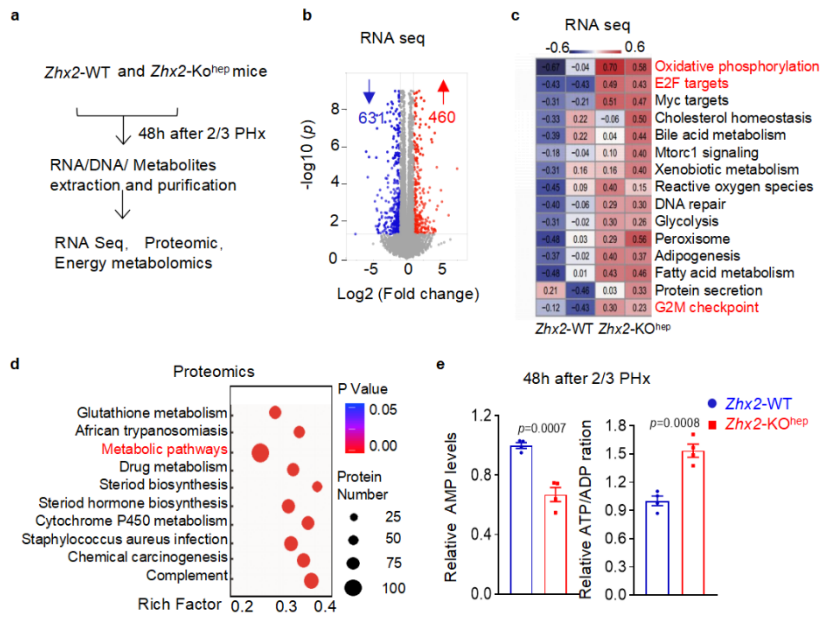
57 old *Zhx2*-WT and *Zhx2*-KO^{hep} mice were determined. Data are presented as mean \pm s.e.m.

58 (Two-tailed Student' s t test. n=5 mice). **c** The protein levels of Cyclin D1, Cyclin A2, Cyclin

59 B1, Cyclin E1 and PCNA were detected in *Zhx2*-WT and *Zhx2*-KO^{hep} mice at indicated time

60 points after 2/3 PHx by western blot (WT: *Zhx2*-WT, KO: *Zhx2*-KO^{hep}). These experiments
61 have been repeated for three times with similar results. **d** Representative images of mitotic
62 hepatocytes (indicated by arrows) of liver sections from *Zhx2*-WT and *Zhx2*-KO^{hep} mice at
63 indicated time points after 2/3 PHx are displayed at left panel. The quantitative data are
64 presented on right panel. Scale bar: 50 μ m. Data are represented as mean \pm s.e.m. (Two-
65 tailed Student' s t test. n=5 mice per group). **e-f** The ALT, AST (e) and H&E (f) were
66 determined in *Zhx2*-WT and *Zhx2*-KO^{hep} mice at 168 h after 2/3 PHx. Scale bar: 100 μ m.
67 Data are presented as mean \pm s.e.m. (Two-tailed Student' s t test. n=4 mice per group). **g-**
68 **h** The liver/body weight ratios (g) and BrdU (h) were determined in *Zhx2*-WT and *Zhx2*-
69 KO^{hep} mice at 36 h and 48 h after sham operation. Scale bar: 50 μ m. Data are presented
70 as mean \pm s.e.m. (Two-tailed Student' s t test. n=3 mice per group). **i** The protein levels of
71 proliferation-related genes, such as CyclinD1, CyclinA2, CyclinB1, Cyclin E1 and PCNA,
72 were detected in the livers of *Zhx2*-WT and *Zhx2*-KO^{hep} mice after CCl4 injection,
73 respectively. These experiments have been repeated for three times with similar results.

74
75
76
77



78

79 **Supplementary Figure 3. Multi-omics analysis reveals enhanced OXPPOS activity in**

80 **hepatocytes with *Zhx2* deficiency during liver repair.**

81 **a** Schematic of the experimental strategy used to identify the potential target of ZHX2 in

82 the samples of *Zhx2*-WT and *Zhx2*-KO^{hep} mice after 2/3 PHx. **b** Volcano plot represented

83 differentially expressed genes between *Zhx2*-WT and *Zhx2*-KO^{hep} mice liver tissues. The

84 significantly up-regulated genes were labeled as red, and the significantly down-regulated

85 genes were labeled as blue. **c** RNA-seq was performed with liver tissues from *Zhx2*-KO^{hep}

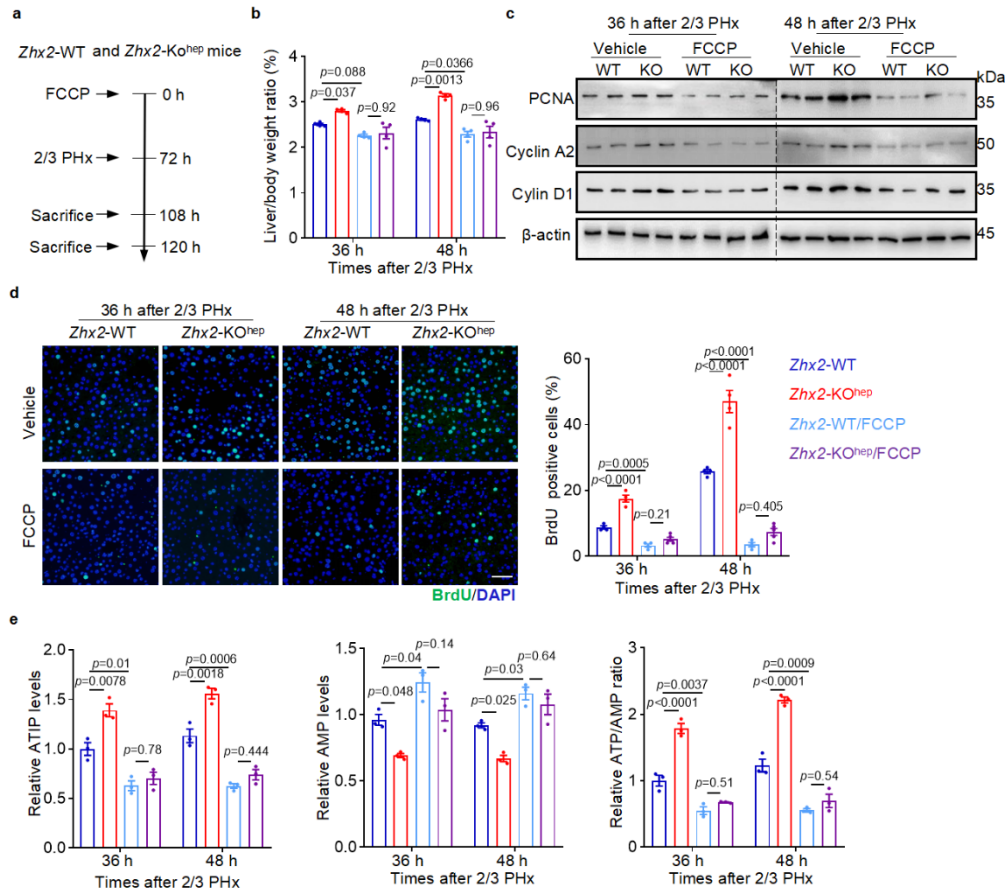
86 and *Zhx2*-WT mice at 48 h after 2/3 PHx. GSEA were used to analyze the genes with

87 differential mRNA levels. **d** KEGG analysis of the differential proteins from *Zhx2*-WT and

88 *Zhx2*-KO^{hep} mice showed top enriched categories. **e** AMP levels and ATP/ADP ratio in

89 hepatocytes from *Zhx2*-KO^{hep} and *Zhx2*-WT mice were accessed. Data are presented as

90 mean ± s.e.m. (Two-tailed Student's t test. n=4 mice per group).



91

92 **Supplementary Figure 4. FCCP treatment abolishes *Zhx2* deletion-induced**
 93 **augmentation of mitochondrial OXPHOS and liver recovery.**

94 **a** Diagram of FCCP administration in *Zhx2*-KO^{hep} and *Zhx2*-WT mice with 2/3 PHx was
 95 presented. **b** Liver/body weight ratios of *Zhx2*-WT and *Zhx2*-KO^{hep} mice with or without
 96 FCCP administration were measured at 36 h and 48 h after 2/3 PHx, respectively. Data are
 97 presented as mean ± s.e.m. (One-way ANOVA with Tukey's test. n=4 mice per group). **c**
 98 Expression of PCNA, Cyclin A2 and Cyclin D1 in *Zhx2*-WT and *Zhx2*-KO^{hep} livers with or
 99 without FCCP treatment were determined at 36 h and 48 h after 2/3 PHx by western blot.
 100 These experiments have been repeated for three times with similar results. **d** BrdU-positive
 101 cells in livers from FCCP and vehicle treated *Zhx2*-KO^{hep} and *Zhx2*-WT mice were
 102 determined, respectively. Representative images (left) and quantitative data (right) were

103 presented. Scale bar: 50 μ m. Data are presented as mean \pm s.e.m. (One-way ANOVA with
104 Tukey's test. n=4 mice per group). **e** ATP and AMP levels, and ATP/AMP ratio of FCCP and
105 vehicle administrated *Zhx2*-KO^{hep} and *Zhx2*-WT livers were determined at 36 h and 48 h
106 after 2/3 PHx. Data are presented as mean \pm s.e.m. (One-way ANOVA with Tukey's test.
107 n=3 mice per group).

108

109

110

111

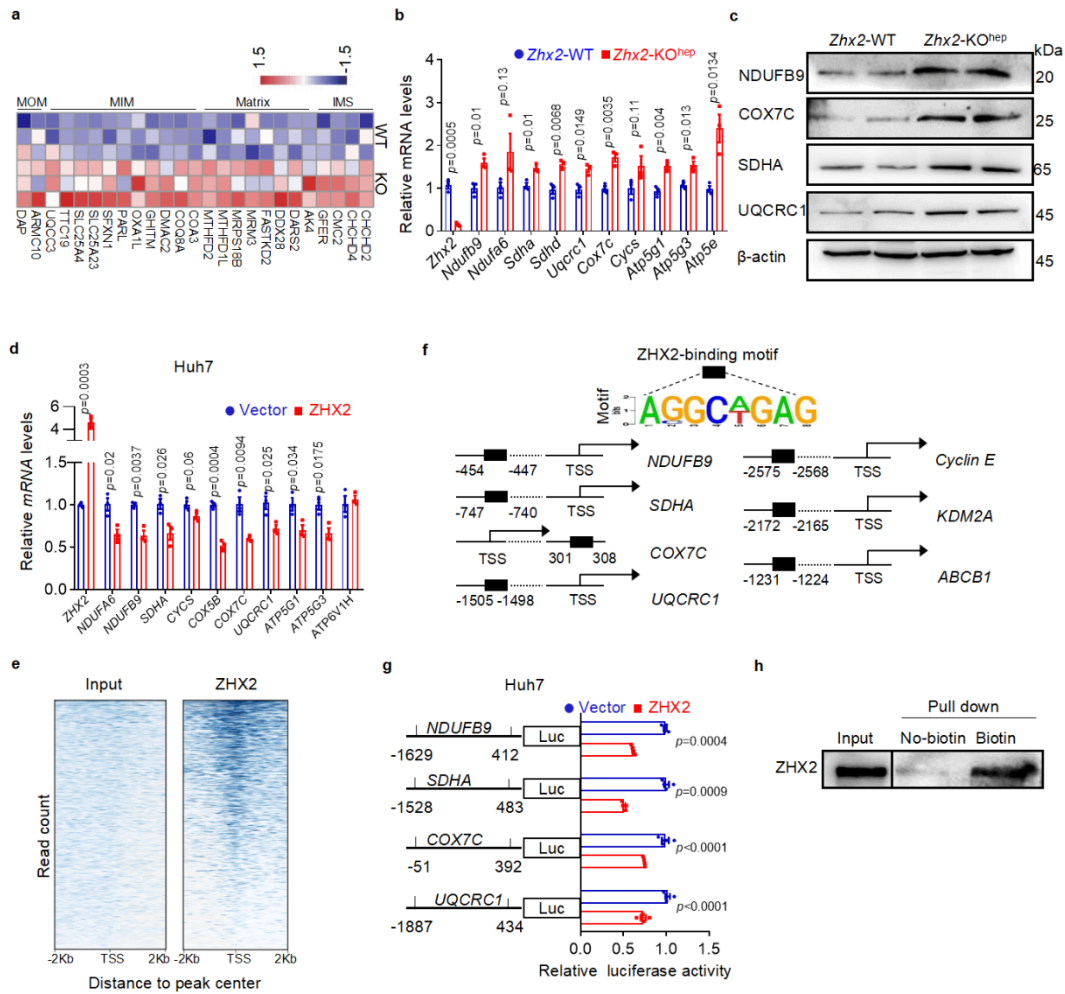
112

113

114

115

116

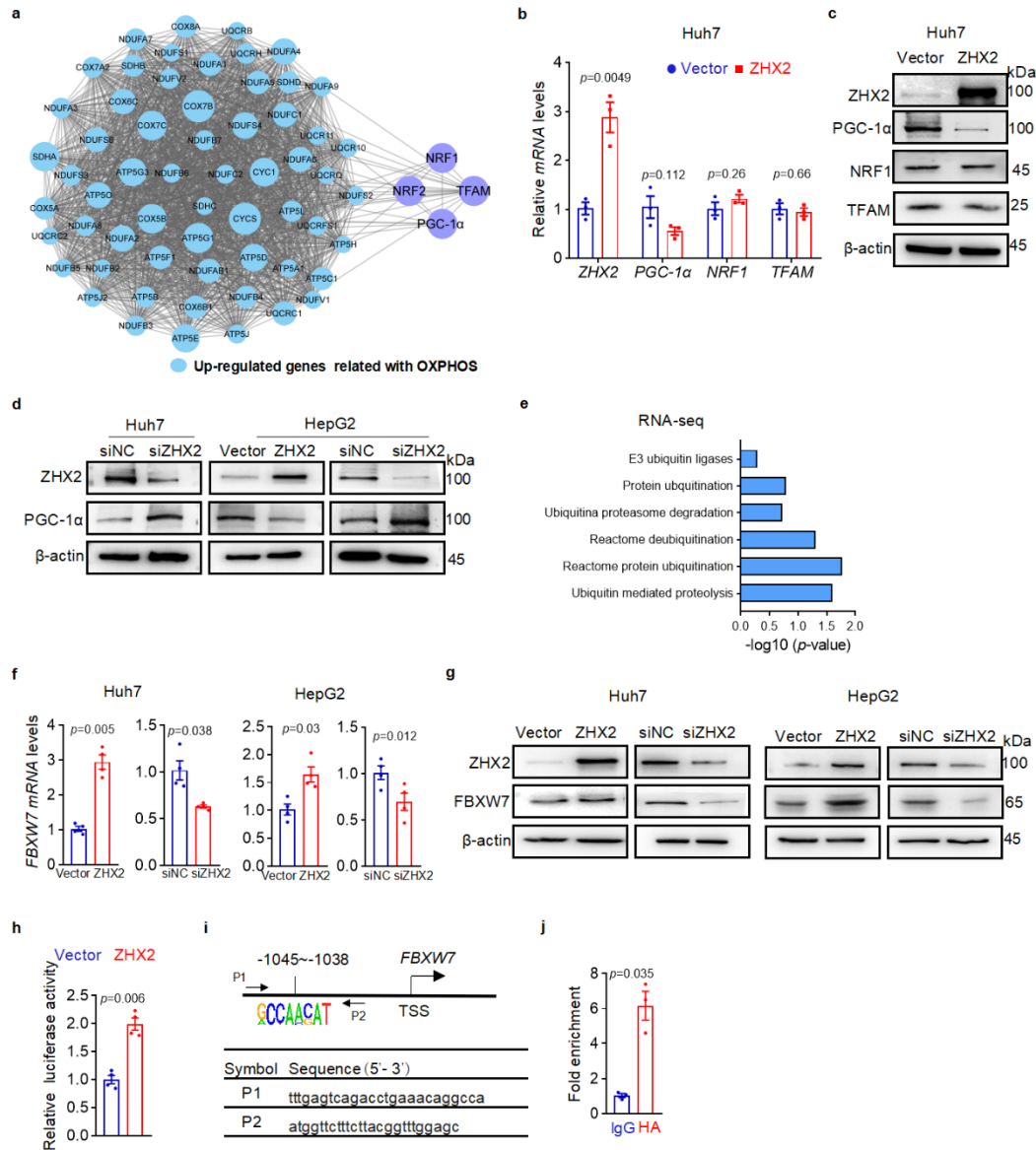


117

118 **Supplementary Figure 5. ZHX2-binding motif is located on the promoter of ETC**
 119 **genes.**

120 **a** Differentially expressed mitochondrial related proteins detected by the proteomics were
 121 presented as heatmap. MOM, mitochondrial outer membrane; MIN, mitochondrial inner
 122 membrane; IMS, intermembrane space. **b** Expression of ETC genes were assessed in
 123 hepatocytes of *Zhx2*-KO^{hep} and *Zhx2*-WT mice at 48 h after 2/3 PHx by RT-qPCR. Data
 124 are presented as mean \pm s.e.m. (Two-tailed Student's t test. n=3 mice per group). **c** The
 125 protein levels of ETC components were assessed in hepatocytes from *Zhx2*-KO^{hep} and
 126 *Zhx2*-WT mice at 48 h after 2/3 PHx by western blot. These experiments have been

127 repeated for three times with similar results. **d** Relative mRNA levels of ETC genes were
128 measured in Huh7 cells with ZHX2 overexpression by RT-qPCR. Representative data are
129 presented as mean \pm sd. (Two-tailed Student' s t test. n=3 biologically independent
130 samples). **e** Heatmap displayed ChIP-Seq signal density for ZHX2 ChIP and input centered
131 on predicted Transcription Start Site (TSS). **f** The diagram shows the sequence of ZHX2-
132 binding putative motif and the location of this motif on the promoter of ZHX2 target genes.
133 **g** The promoter activity of indicated ETC genes were determined in Huh7 cells with or
134 without ZHX2 overexpression by dual-luciferase assays. The schematic representation of
135 the promoter regions for ETC genes were displayed on the left. Representative data are
136 presented as mean \pm sd. (Two-tailed Student' s t test. n=4 biologically independent
137 samples). **h** Biotin-labeled ZHX2-binding motif (probe) was incubated with nuclear protein
138 of Huh7 cells with ZHX2 overexpression to validate the binding of ZHX2 with the consensus
139 motif.

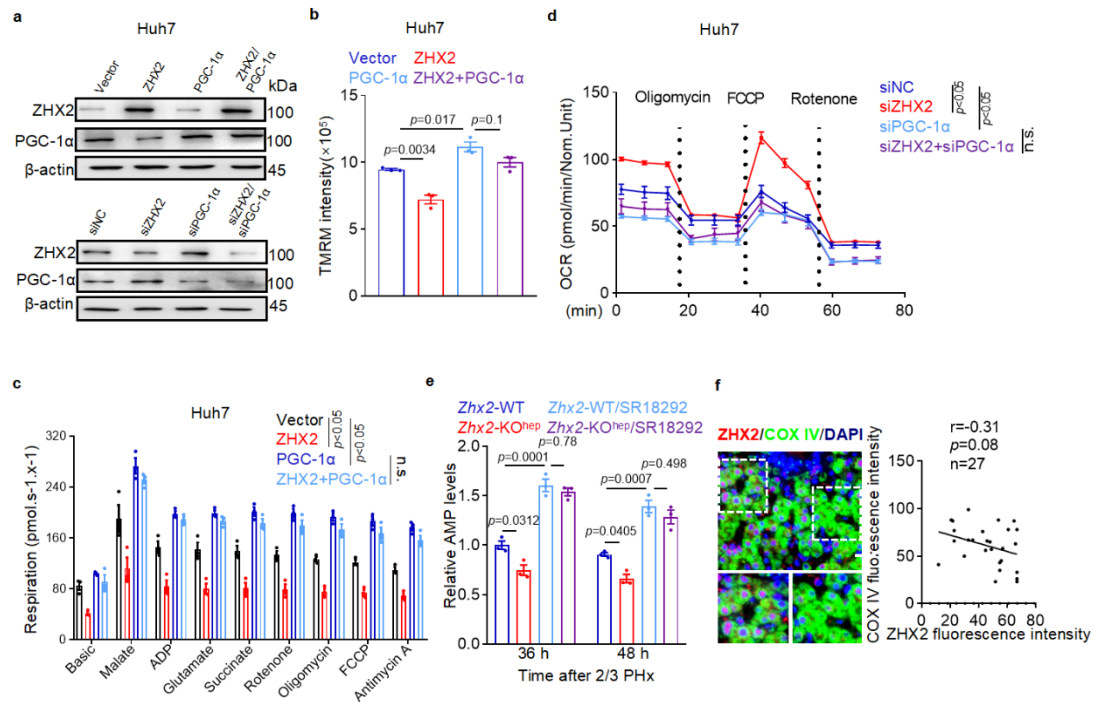


140

141 **Supplementary Figure 6. ZHX2 decreases PGC-1α protein levels through up-**
 142 **regulation of FBXW7.**

143 **a** The relationship of mitochondrial regulators (PGC-1α, NRF1/2 and TFAM)-
 144 regulated mitochondrial OXPHOS genes were analyzed by co-expression network. **b** The
 145 mRNA levels of *PGC-1α*, *NRF1* and *TFAM* were detected in ZHX2 and control vectors
 146 transfected Huh7 cells by RT-qPCR. Representative data are presented as mean ± sd.
 147 (Two-tailed Student' s t test. n=3 biologically independent samples). **c** The protein levels

148 of PGC-1 α , NRF1 and TFAM in Huh7 cells transfected with ZHX2 and control vector were
149 detected by western blot. These experiments have been repeated for three times with
150 similar results. **d** The expression of PGC-1 α were detected in Huh7 and HepG2 cells with
151 ZHX2 manipulation by western blot. **e** GSEA analysis showed the enrichment of
152 differentially expressed ubiquitination related gene sets in *Zhx2*-KO^{hep} mice at 48 h after
153 2/3 PHx. **f** Relative mRNA levels of FBXW7 in Huh7 and HepG2 cells with ZHX2
154 overexpression or knockdown were measured by RT-qPCR, respectively. Representative
155 data are presented as mean \pm sd. (Two-tailed Student' s t test. n=4 biologically
156 independent samples). **g** The expression of FBXW7 were detected in ZHX2-manipulated
157 Huh7 and HepG2 cells by western blot. These experiments have been repeated for three
158 times with similar results. **h** The luciferase reporter vector containing FBXW7 promoter was
159 co-transfected with ZHX2-HA or control vectors in Huh7 cells. The promoter activities were
160 displayed as the luciferase intensity. Representative data are presented as mean \pm sd.
161 (Two-tailed Student' s t test. n=4 biologically independent samples). **i** The upper panel
162 showed location of ZHX2-binding motif on FBXW7 promoter detected in the ChIP-Seq data.
163 The bottom panel showed primer sequences for ChIP assays. **j** ChIP assay was performed
164 with anti-HA antibody, IgG as control, using Huh7 cells transfected with ZHX2-HA. ZHX2
165 occupied at the promoter of FBXW7 was quantified by qPCR. Representative data are
166 presented as mean \pm sd. (Two-tailed Student' s t test. n=3 biologically independent
167 samples).



168

169 **Supplementary Figure 7. Loss of *Zhx2* enhances mitochondrial OXPHOS by**
 170 **stabilization of PGC-1α.**

171 **a** The protein levels of PGC-1α and ZHX2 were detected in Huh7 cells with ZHX2/PGC-1α
 172 overexpression or knockdown by western blot, respectively. These experiments have been
 173 repeated for three times with similar results. **b** The fluorescence intensity of TMRM were
 174 analyzed in Huh7 cells with indicated manipulation by flow cytometry. The quantitative data
 175 were presented. Representative data are presented as means ± sd. (One-way ANOVA
 176 with Tukey's test. n=3 biologically independent samples). **c** Oxygen consumption was
 177 analyzed in Huh7 cells with indicated manipulation by oxygraph-2k assay kit.
 178 Representative data are presented as means ± sd. (One-way ANOVA with Tukey's test.
 179 n=3 biologically independent samples. n.s. indicates the difference is not significant). **d**
 180 Oxygen consumption was analyzed in Huh7 cells with indicated manipulation by using
 181 seahorse analyzer. Representative data are presented as means ± sd. (Two-tailed Student'

182 s t test. n=4 biologically independent samples. n.s. indicates the difference is not
183 significant). **e** AMP levels of vehicle or 18292 treated *Zhx2*-WT and *Zhx2*-KO^{hep} mice liver
184 were determined at 36 h and 48 h after 2/3 PHx. Data are presented as mean \pm s.e.m.
185 (*One-way ANOVA with Tukey's test. n=3 mice per group). **f** Correlation analysis of
186 fluorescence intensity of ZHX2 and COX IV in DILI patients. Right, representative images.
187 Left, quantitative data. Scale bar: 20 μ m. Pearson's correlation coefficients (*r*) and *p* values
188 (*p*) for two-sided correlation tests are shown.

189

190

191

192

193

194

195

196

197

198

199

200

201

202

203 **Supplementary tables**

204 **Supplementary Table 1 Characteristics of DILI patients**

	All patients	Hepatocellular injury	Cholestatic injury	Mixed injury
n	27	17	3	7
Age (years)	48.48±12.83	46.88±14.20	50.00±17.44	51.71±7.34
Gender (F/M)	16/11	9/8	2/1	5/2
ALT (U/L)	228.45±284.83	293.95±339.53	44.60±49.38	148.16±82.12
AST (U/L)	224.59±269.27	269.44±312.51	63.30±7.18	184.80±182.1
GGT (U/L)	265.59±303.01	285.10±331.16	276.73±407.80	213.43±213.6
ALP (U/L)	154.29±97.82	162.34±110.82	139.50±81.67	141.07±77.44
TBIL	104.09±131.29	72.88±96.71	160.77±173.05	155.59±179.7
TBA	91.03±102.12	88.66±85.42	100.73±96.29	92.64±150.26
<i>Severity, n</i>				
Mild/Moderate	13	7	3	3
Severe/Fatal	14	10	0	4

205 ALP alkaline phosphatase, ALT alanine aminotransferase, AST aspartate
 206 aminotransferase, GGT gamma glutamyl transferase, TBIL total bilirubin, TBA total bile
 207 acid. Data are expressed as mean ± SD.

208

209

210

211

212

213

214

215 **Supplementary Table 2**216 **Synthetic Oligonucleotides.**

Primer for RT-qPCR	
Symbol	Sequence (5' - 3')
h-ZHX2-F	GGTTCGGACATCACAAGTAGTAG
h-ZHX2-R	GGTGTGCCGATTCCCTTTCTCT
h- β -actin-F	AGTTGCGTTACACCCTTTC
h- β -actin-R	CCTTCACCGTTCCAGTTT
h-NDUFB9-F	CTGGGAACGAGAGGTTAAGCA
h-NDUFB9-R	GGGTCTGGTCACAATATAACCACC
h-SDHA-F	CAGCATGTGTTACCAAGCTGT
h-SDHA-R	GGTGTCGTAGAAATGCCACCT
h-UQCRC1-F	GGGGCACAAGTGCTATTGC
h-UQCRC1-R	GTTGTCCAGCAGGCTAACC
h-COX7C-F	GGTCCGTAGGAGCCACTATGA
h-COX7C-R	GTGTCTTACTACAAGGAAGGGTG
h-ATP6V1H-F	GCAAAGAACAGACCGTTCAGT
h-ATP6V1H-R	ATTGGCAGAAAGTAGGGCCAC
h-NDUFA6-F	CGCCAAGCTACTTCTACCGC
h-NDUFA6-R	TCGGACTTTATCCCGTCCCA
h-CYCS-F	CTTTGGGCGGAAGACAGGTC
h-CYCS-R	TTATTGGCGGCTGTGTAAGAG
h-COX5B-F	TGTGAAGAGGACAATACCAGCG
h-COX5B-R	CCAGCTTGTAATGGGCTCCAC
h-ATP5G1-F	TTCCAGACCAGTGTTGTCTCC
h-ATP5G1-R	GACGGGTTCTGGCATAGC
h-ATP5G3-F	CCAGAGTTGCATACAGACCAAT
h-ATP5G3-R	CCCATTAAATACCGTAGAGCCCT
h-PGC-1 α -F	CCAAAGGATGCGCTCTCGTTCA

h-PGC-1 α -R	CGGTGTCTGTAGTGGCTTGACT
h-NRF1-F	AGGAACACGGAGTGACCCAA
h-NRF1-R	TATGCTCGGTGTAAGTAGCCA
h-TFAM-F	GTGGTTTTTCATCTGTCTTGGCAAG
h-TFAM-R	TTCCCTCCAACGCTGGGCAATT
h-ND1-F	CCCTAAAACCCGCCACATCT
h-ND1-R	GAGCGATGGTGAGAGCTAAGGT
h-B2M-F	CCAGCAGAGAATGGAAAGTCAA
h-B2M-R	TCTCTCTCCATTCTTCAGTAAGTCAACT
h-FBXW7-F	GGCGCCGCGGCTCTTTTCTA
h-FBXW7-R	GCTGCCACAGAGAGCAGTTCC
h-RNF34-F	GGAGAGCTTATGGATGGAGACC
h-RNF34-R	GGTCCGATCCTCTGCGTT
m-ZHX2-F	TGGAAGCGAGGCGGCACATCAG
m-ZHX2-R	CCGGCTCCAGCTACCCCACTTCTC
m- β -actin -F	TGCGTGACATCAAAGAGAAG
m- β -actin -R	TCCATACCCAAGAAGGAAGG
m-Cyclin A2-F	ACAGAGTGTGAAGATGCCCTGGCT
m-Cyclin A2-R	AGCATGTGGTGATTCAAAACTGCCA
m-Cyclin B1-F	AAGGTGCCTGTGTGTGAACC
m-Cyclin B1-R	GTCAGCCCCATCATCTGCG
m-Cyclin D1-F	GCGTACCCTGACACCAATCTC
m-Cyclin D1-R	CTCCTCTTCGCACTTCTGCTC
m-Cyclin E1-F	GTGGCTCCGACCTTTCAGTC
m-Cyclin E1-R	CACAGTCTTGTCATCTTGGCA
m-NDUFB9-F	AAGGTGCTGCGGCTGTATAAG
m-NDUFB9-R	TCATCAAGCAAGCAAAGTACCG
m-SDHA-F	GGAACACTCCAAAAACAGACCT
m-SDHA-R	CCACCACTGGGTATTGAGTAGAA
m-SDHD-F	TGGTCAGACCCGCTTATGTG

m-SDHD-R	GAGCAGGGATTCAAGTACCCA
m-UQCRC1-F	AGACCCAGGTCAGCATCTTG
m-UQCRC1-R	GCCGATTCTTTGTTCCCTTGA
m-COX7C-F	ATGTTGGGCCAGAGTATCCG
m-COX7C-R	ACCCAGATCCAAAGTACACGG
m-ATP5G1-F	TTCTCCAGCTCTGATTGCTC
m-ATP5G1-R	CCGGGAAATGACACTGGTCT
m-ATP5G3-F	CTGGTATTGGAACAGTCTTTGGC
m-ATP5G3-R	GATCAAGAACGCAACCATCAAAC
m-ATP5B-F	TCCTGCCAGAGACTATGCG
m-ATP5B-R	GATGACTGCCACGATTGCG
m-D-loop-F	AATCTACCATCCTCCGTGAAACC
m-D-loop-R	TCAGTTTAGCTACCCCAAGTTTAA
m-B2M-F	ATGGGAAGCCGAACATACTG
m-B2M-R	CAGTCTCAGTGGGGGTGAAT
m-NDUFA6-F	TCGGTGAAGCCCATTTTCAGT
m-NDUFA6-R	CTCGGACTTTATCCCGTCCTT
m-CYCS-F	CCAAATCTCCACGGTCTGTTC
m-CYCS-R	ATCAGGGTATCCTCTCCCCAG
m-FBXW7-F	GTTCCGCTGCCTAATCTTCCT
m-FBXW7-R	CCCTTCAGGGATTCTGTGCC
m-RNF34-F	GAAACATACCAACCGACACTTGT
m-RNF34-R	AGGCTACTTGAGTCCAGGTCA

Primer for ChIP-PCR

Symbol	Sequence (5'- 3')
NDFB9-ChIP-F	CTCCACCAGATGGTGATGAC
NDFB9-ChIP-R	ATTCATCCCACGTGCACCT
SDHA-ChIP-F	CACCGGACACTTTCATATGAGCTAGG
SDHA-ChIP-R	GTTTGCACCTTCCCCACATCAC
COX7C-ChIP-F	CTGTGACTCGCGCACCT

COX7C-ChIP-R	CGCTAGGATGCCAGCT
UQCRC1-ChIP-F	AAATAAAGTCAGCCTGGCACGG
UQCRC1-ChIP-R	ATGTTGCCAGGCTGATCTTAAAC

Synthetic interfering RNA

Symbol	Sequence (5' - 3')
Scramble-sense	UUCUCCGAACGUGUCACGUTT
Scramble-antisense	ACGUGACACGUUCGGAGAATT
homo-ZHX2-1-sense	GCAGAACUGGAUCGGCUAATT
homo-ZHX2-1-antisense	UUAGCCGAUCCAGUUCUGCTT
homo-ZHX2-2-sense	CGAGGAGUCGAGCGUUGTGTT
homo-ZHX2-2- antisense	CACAACGCUCGACUCCUCGTT
homo-PGC-1 α -1-sense	GUCGCAGUCACAACACUUATT
homo-PGC-1 α -1-antisense	UAAGUGUUGUGACUGCGACTT
homo-PGC-1 α -2-sense	GUGUGAUUUUAUGUCGGUAATT
homo-PGC-1 α -2-antisense	UUACCGACAUAAAUCACACTT
homo-FBXW7-sense	ACAGGACAGUGUUUACAAATT
homo-FBXW7-antisense	UUUGUAAACACUGUCCUGUTT

217

218

219